Unclassified
SECURITY CLASSIFICATION OF THIS PAGE

DTIC FILE COPY (2)

REPORT DOCUMENTATION PAGE

Form Approved OMB No. 0704-0188

AD-A219 315

DTIC ELECTE JAN 26 1990 B

	1b. RESTRICTIVE MARKINGS
	3. DISTRIBUTION/AVAILABILITY OF REPORT Approved for public release; distribution is unlimited.
4. PERFORMING ORGANIZATION REPORT NUMBER(S)	5. MONITORING ORGANIZATION REPORT NUMBER(S) AFOSR-TR- 90-0191
6a. NAME OF PERFORMING ORGANIZATION Nielsen Engineering & Research Inc.	6b. OFFICE SYMBOL (If applicable) N/A
7a. NAME OF MONITORING ORGANIZATION AFOSR/NA	
6c. ADDRESS (City, State, and ZIP Code) 510 Clyde Avenue Mountain View, CA 94043-2287	7b. ADDRESS (City, State, and ZIP Code) Building 410, Bolling AFB DC 20332-6448
8a. NAME OF FUNDING/SPONSORING ORGANIZATION AFOSR/NA	8b. OFFICE SYMBOL (If applicable) NA
9. PROCUREMENT INSTRUMENT IDENTIFICATION NUMBER F49620-88-C-0003	
8c. ADDRESS (City, State, and ZIP Code) Building 410, Bolling AFB DC 20332-6448	10. SOURCE OF FUNDING NUMBERS PROGRAM ELEMENT NO. 61102F; PROJECT NO. 2308; TASK NO. A2; WORK UNIT ACCESSION NO.

11. TITLE (Include Security Classification)
(U) The Effects of Compressibility on a Supersonic Mixing Layer (Unclassified)

12. PERSONAL AUTHOR(S)
Nixon, D., Keefe, L. R., and Kuhn, G. D.

13a. TYPE OF REPORT	13b. TIME COVERED	14. DATE OF REPORT (Year, Month, Day)	15. PAGE COUNT
Annual	FROM 12/1/88 TO 11/30/89	1989 December 28	22

16. SUPPLEMENTARY NOTATION

17. COSATI CODES			18. SUBJECT TERMS (Continue on reverse if necessary and identify by block number)
FIELD	GROUP	SUB-GROUP	mixing layers, compressible flow

19. ABSTRACT (Continue on reverse if necessary and identify by block number)

The objective of the work is to identify the flow mechanisms that cause the decrease in spreading rate of supersonic mixing layers as the convective Mach number increases and to suggest means of enhancing the mixing. Two approaches have been taken, one numerical and one analytic. A computer code, TMRC, has been used to simulate both time and space developing mixing layers to get some indication of the flow physics. To complement the numerical study a simple analysis has been developed which explains the variation of mixing rate with convective Mach number. The analysis seems to indicate that little can be done to enhance mixing as such although the real problem of simultaneous mixing and combustion may be more amenable to control.

20. DISTRIBUTION/AVAILABILITY OF ABSTRACT	21. ABSTRACT SECURITY CLASSIFICATION
☒ UNCLASSIFIED/UNLIMITED ☒ SAME AS RPT. ☐ DTIC USERS	Unclassified
22a. NAME OF RESPONSIBLE INDIVIDUAL Julian M Tishkoff	22b. TELEPHONE (Include Area Code) (202) 767-0465
	22c. OFFICE SYMBOL AFOSR/NA

DD Form 1473, JUN 86 Previous editions are obsolete. SECURITY CLASSIFICATION OF THIS PAGE

Unclassified

THE EFFECTS OF COMPRESSIBILITY ON A SUPERSONIC MIXING LAYER

AFOSR Contract No. F49620-88-C-0003

Principal Investigator: David Nixon

Nielsen Engineering & Research, Inc.
510 Clyde Avenue
Mountain View, CA 94043-2287

ABSTRACT

The objective of the work is to identify the flow mechanisms that cause the decrease in spreading rate of supersonic mixing layers as the convective Mach number increases and to suggest means of enhancing the mixing. Two approaches have been taken, one numerical and one analytic. A computer code, TMRC, has been used to simulate both time and space developing mixing layers to get some indication of the flow physics. To complement the numerical study a simple analysis has been developed which explains the variation of mixing rate with convective Mach number. The analysis seems to indicate that little can be done to enhance mixing as such although the real problem of simultaneous mixing and combustion may be more amenable to control.

Research Objectives

The overall objective is to identify the flow mechanisms that cause the decrease in the spreading rate of supersonic mixing layers and to suggest means of enhancing the mixing.

In the past year the objective has been to extend and consolidate the simple theory developed in the first year of the contract and to see if it provides some insight in enhancement of mixing. This study is augmented by the development of a computer code to numerically simulate the temporally and spatially developing mixing layers to gain insight into the physics of the flow.

Status of the Research Effort

At the end of the first year of the contract a simple theory had been developed of the spreading rate variation with convective Mach number. This theory is based on the transonic small disturbance equation (Ref. 1)

$$(\beta^2 - k\phi_x)\phi_{xx} + \phi_{yy} = M_c^2 \phi_{tt} + 2M_c^2 \phi_{xt} \qquad (1)$$

where ϕ is a perturbation velocity potential, t is time nondimensionalized by c/U_c where c and U_c are characteristic length and convective velocity respectively, and M_c is the convective Mach number.

$$\beta^2 = 1 - M_c^2$$

$$k = (\gamma+1)M_c^2 \tag{2}$$

The nondimensionalized mixing, $\bar{m}$, is related to its value at incompressible ($M_c = 0$) mixing, $\bar{m}_i$, by

$$\frac{\bar{m}}{\bar{m}_i} = \left(\frac{\bar{m}_o}{\bar{m}_{oi}}\right)^2 \left[(RKE)_{oi}/(RKE)\right] \tag{3}$$

where $\bar{m}_o$ is the nondimensional mixing associated with a rotational kinetic energy (RKE) of $(RKE)_o$ at a convective Mach number of M_c.

If $M_c << 1$, the Prandtl-Glauert equation ($k = 0$) may be used and Equation (3) becomes

$$\frac{\bar{m}}{\bar{m}_i} = \beta^3/(1 - M_c^2/2) \tag{4}$$

The results predicted by this theory show good agreement with experimental data, see Figure 1, especially for $M_c < 0.7$.

At the end of the first reporting period it was concluded that mixing is reduced because the eddies produced a decrease in size as M_c increases. In the last year it has been shown that this conclusion is wrong.

Over the last year the theory has been consolidated, that is, fewer assumptions are made, and has been extended to include three-dimensional effects. A full description of the theory is given in the Appendix, which is AIAA Paper 90-0706. A summary of the main findings is given below.

(a) No matter the size or number of spanwise vortices, the mixing will decrease with increasing M_c at the same rate. This indicates that two-dimensional eddy break up devices may not work.

(b) Streamwise vortices will not be affected by M_c to a first approximation and the mixing associated with these vortices is unchanged with M_c.

(c) If the hypothesis is made that large fluid mechanical structures, such as vortices, will deform to avoid shock waves, then the theory is greatly improved (Figure 1). The deformation may consist of vortex sweep, rather like a swept wing or a bifurcation, rather like the braids commonly seen in incompressible mixing layers. This hypothesis, if true, would have considerable implications in other fluid mechanics problems.

(d) Since the present theory is based on notions of irrotational flow it suggests that other studies based on vorticity redistribution arguments are erroneous. It may also be suggested that since the present theory is based on nonlinear finite disturbances, explanations of the phenomena based on linear stability theory are irrelevant. This latter viewpoint is corroborated by the fact that experimental data are taken a considerable distance downstream of the region where linear instability theories are valid.

(e) The main cause of the decrease in mixing as M_c increases is that an increasing amount of the energy in the two streams goes into compression of the fluid during entrainment rather than being used to produce pure mixing. The only way to increase mixing is to accentuate streamwise vorticity and, if the hypothesis in (c) is valid, Nature is doing its best to achieve this goal.

In addition to the theory given in the Appendix numerical simulations of both time and space evolving mixing layers have been performed. The code used is TMRC which is a fourth order accurate code developed at Nielsen Engineering & Research (NEAR) for impinging jet flows. These calculations were performed to get some insight into two-dimensional mixing layers; a typical example of such a calculation is shown in Figure 2. At present the numerical results are similar to those obtained by other investigators. Attempts to avoid duplication by obtaining the computer code developed by NASA Ames Research Center to study mixing layers proved fruitless on the grounds that the code was not ready for public use.

Written Publications

Nixon, D., Keefe, L. R., and Kuhn, G. D., The Effects of Compressibility on a Supersonic Mixing Layer, AIAA Paper 90-0706, 1990.

Professional Personnel

Dr. David Nixon
Dr. Laurence R. Keefe
Dr. Gary D. Kuhn

Interactions

(a) An early version of the theory was presented at the AFOSR/ONR contractors meeting in Ann Arbor, Michigan in June 1989.

(b) Extensive discussions about the theory were conducted with Professor Peter Bradshaw of Stanford University, June 1989.

(c) Discussions on the theory with Dr. Richard Rivir of Air Force Propulsion Laboratory, October 1989.

(d) Invited seminar on theory to Minnesota Supercomputer Center, October 18, 1989; cancelled on day of lecture due to San Francisco earthquake; rescheduled for April 25, 1990.

(e) Paper on theory to be presented at AIAA Aerospace Sciences Meeting, Reno, Nevada, January 1990.

(f) Discussion on validity of the hypothesis noted in section (c) of "Status of the Research Effort" with Professor Max Platzer of Naval Postgraduate School, Monterey, CA, with emphasis on relevance to dynamic stall, November 1989.

(g) Discussions in October 1989 on validity of hypothesis in section (c) of "Status of the Research Effort" and other aspects of mixing layers with Mr. Richard Dix of AEDC, Tullahoma, TN, with application to the flow in weapons bays.

Discoveries

No new discoveries or patents have resulted from this work.

Reference

1. Nixon, D. (editor): Transonic Aerodynamics, Prog. in Astro and Aero., Vol. 81, 1983.

2. Papamoschou, D. and Roshko, A.: Observation of Supersonic Free Shear Layers, AIAA 86-0162, January 1986, Reno, Nevada.

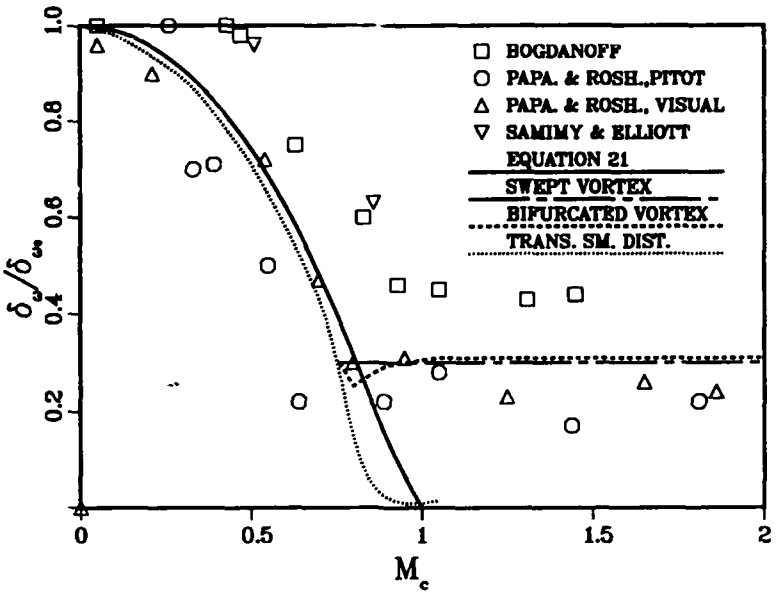

FIGURE 1. Experimentally measured layer growth rates compared to two– and three–dimensional theory.

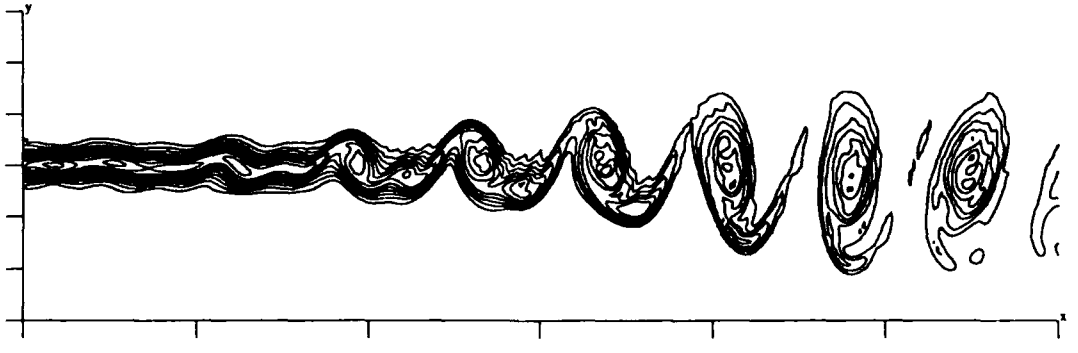

FIGURE 2. Vorticity contours in a two–dimensional mixing layer. $M_1 = 2.0$, $M_2 = 1.2$, $M_c = .4$.

APPENDIX

The Effects of Compressibility On a Supersonic Mixing Layer

by

David Nixon
Laurence R. Keefe
Gary D. Kuhn

Nielsen Engineering & Research, Inc
510 Clyde Avenue
Mountain View, CA 94043-2287

THE EFFECTS OF COMPRESSIBILITY ON A SUPERSONIC MIXING LAYER

David Nixon*
Laurence R. Keefe**
Gary D. Kuhn***

Nielsen Engineering & Research, Inc.
510 Clyde Avenue
Mountain View, CA 94043-2287

ABSTRACT

A theory that predicts the observed decrease of mixing in a compressible shear layer with respect to its incompressible counterpart at the same density and velocity ratios is described. Unlike previous investigations, it does not attribute this decrease to the reduction in growth rates calculated from linear instability analysis of compressible shear layers. Rather a two part transonic theory is offered. At lower convective Mach numbers, the asymptotic mixing rate is calculated analytically by relating it to the mixing and energy of an isolated vortex, and then replacing that with the bound circulation of a two-dimensional transonic airfoil. At higher convective Mach numbers the mixing rate is well described by assuming an increasing three-dimensionality of the vortices that delays the appearance of shock waves. This three-dimensionality can be represented either by swept vortices or by assumption of a bifurcation in which longitudinal vortices become increasingly important.

INTRODUCTION

Compressible mixing layers barely live up to their name. To the dismay of supersonic combustor designers, adjacent streams of differing, high speed, compressible fluids mix much slower at their interface than the same fluids at low speeds and the same velocity and density ratios. This effect was demonstrated conclusively in the experiments of Papamoschou and Roshko,[1] who correlated shear layer spreading rate data from theirs and earlier studies using the convective Mach number (M_c) concept introduced by Bogdanoff.[2] Since then other experiments[3,4,5] have further documented this effect both in plane and circular shear layers. Density differences between the streams were originally suggested as the cause of this mixing decrease, but the work of Brown and Roshko[6] showed this not to be the case. More recently this phenomenon has been attributed to the decrease with Mach number of linear instability growth rates calculated for supersonic shear layers.[7,8] Lele[9] has provided a physical explanation for the attenuation of linear instability by pointing out the retarding effects of velocity divergence and baroclinic torques in the initial vorticity redistribution process.

While the similarities between linear growth reduction and mixing rate decrease are suggestive, positing a cause and effect relation between them ignores a simple experimental fact: measured mixing rates are obtained in fully turbulent regions of the flow, far downstream of stations where linear instability is the dominant mechanism. The often cited measurements of Papamoschou and Roshko derived mixing rates from stations greater than 1000 θ, where θ is the trailing edge boundary layer thickness on the high speed side. For this region they state (p. 462, Ref. 1): "Given that the shear layer is fully turbulent, we expect it to grow linearly." The recent measurements of Samimy and Elliot[3] were obtained from flows where the trailing edge boundary layers were fully turbulent, and still they deduced the mixing rates from stations at least twice the distance downstream from where their measurements show the turbulent shear layer to be fully established. The spatially developing numerical simulations of Lele begin with a forced laminar *tanh* profile, whose development is only followed for some 200 initial layer thicknesses δ_{ω_o}. Growth rates are displayed for only the initial 60 δ_{ω_o} before pairing even occurs. Thus while instability theory and experiments show similar trends, the flow regimes of the two cases are not the same.

In the following sections we describe a theory appropriate for the asymptotic mixing rate of compressible shear layers; it does not depend on linear instability arguments. We first derive an expression for the energy within a control volume circumscribing a portion of the turbulent shear layer, in terms of the mixing rate (rate of increase of mass within the volume) and convective Mach number M_c. We then show that the mixing rate of an isolated vortex is proportional to the square root of its energy and thus establish a scaling between the mixing rate due to an arbitrary vortex and that of a reference vortex, based on the ratio of their energies. Identifying the energy and mixing rate of the

*President
**Sr. Research Scientist
***Sr. Research Scientist. Associate Fellow AIAA

control volume analysis with that of an arbitrary vortex yields a relation between the nondimensionalized mixing in the shear layer and the energy and mixing due to a reference, isolated vortex sitting in a uniform free stream of Mach number M_c.

The reference vortex is then taken to be the bound circulation of a lifting airfoil. Both the mixing and energy of this reference "vortex" can be calculated analytically from solution of the Prandtl-Glauert equation with $M_\infty = M_c$. The resulting expression for the shear layer mixing as a function of M_c agrees well with experimental data for $M_c \leq M^* \sim .77$. Above this critical value of M_c we theorize that three-dimensional effects become more important, and that the flow evolves to avoid shocks. One configuration that accomplishes this assumes the spanwise vortices acquire a sweep angle just sufficient to keep velocities subsonic. Another possible configuration echoes the roller and braid structure of incompressible layers. Here the spanwise vortex decays to avoid shocks, but the streamwise vortex increases in strength. In either case, simple modifications to the original analysis show the normalized mixing rate to remain essentially constant at its value at M_c^*, again in agreement with experimental data.

The physical configuration of a compressible free shear layer is shown in Figure 1, where ω_z vorticity contours have been drawn from the results of our own two-dimensional direct numerical simulations of this flow. These simulations integrate the Navier-Stokes equations using standard fourth-order finite volume spatial discretization, fourth-order Runge-Kutta time advance, and "characteristic" boundary conditions due to Thompson[10] at the outflow and upper and lower boundaries. Two parallel streams, initially separated by a splitter plate, and semi-infinite in directions transverse to the mean flow, mix at their interface. The upper stream is characterized by ρ_1, U_1, a_1, and the lower by ρ_2, U_2, a_2 ($U_1 \geq U_2$ assumed). Static pressures in the stream are matched at the trailing edge of the splitter plate so that no expansion/compression waves contaminate the streamwise development of the flow. Initial instability of this shear layer causes it to roll up into spanwise vortices which subsequently pair due to a further spatial subharmonic instability. As the roll-up and growth of vortices proceeds, the width of the shear layer grows downstream, and increasing amounts of fluid are entrained from both sides. The growth rate of incompressible shear layers depends on their velocity and density ratios. High speed shear layers, however, grow much more slowly than their incompressible counterparts at the same velocity and density ratios. Bogdanoff, and later Papamoschou and Roshko, suggested that the effect of compressibility on growth of a shear layer is characterized by Mach numbers M_{c_i} measured relative to the convective speed U_c of the large structures. Thus

$$M_{c_1} = \frac{U_1 - U_c}{a_1}, \qquad M_{c_2} = \frac{U_c - U_2}{a_2} \quad . \quad (1)$$

A relation between M_{c_1} and M_{c_2} is obtained by assuming that the two streams have equal static pressures, and that their stagnation values in the U_c reference frame are also equal. If it is further assumed that the ratio of specific heats γ_i for each stream is equal, then $M_{c_1} = M_{c_2} = M_c$, and the convective velocity may be calculated as a sound speed weighted average

$$U_c = \frac{a_2 U_1 + a_1 U_2}{a_1 + a_2} \quad .$$

Although there is some scatter, all experimental evidence supports this claim, and numerical simulations by Lele[9] have shown that pressure maxima (stagnation points) and minima (structure centers) do travel at U_c in the initial part of the layer. The decrease in growth rate as M_c increases can be seen in Figure 2, where the thickness of three shear layers at $M_c = .4, .6, .7$ are plotted versus downstream distance. The width measure used is the vorticity thickness.

$$\delta_\omega(x) = (U_1 - U_2) \Big/ \left. \frac{\partial U(x,y)}{\partial y} \right|_{max}$$

CONTROL VOLUME ANALYSIS

Refer again to Figure 1 and the control volume drawn about a portion of the flow. The volume moves at U_c, the velocity of the large structures, and is assumed to contain at least one of them. The upper and lower boundaries are sufficiently far from the interface that we assume no vertical velocity on them. Then the idealized model of the mixing layer is shown in Figure 3, where flow variables U, ρ, p, etc., are subscripted according to the volume (V_1, V_2) they are associated with, and quantities topped by a tilde (~) refer to average quantities in similarity variables on the segments AD and BC.

In Figure 3 the difference between fluid entering AD and leaving BC is mixed fluid that is a consequence of a "mixer" in V_o. While it is helpful to think of the mixer as a vortex, this assumption is not essential to the analysis. The change in energy flux between AD and BC will be proportional to the energy in the mixer, since the increase is due solely to a thickening of the mixing layer, when the flow on AD and BC is similar. This has been found to be true in experiments if one is in the

asymptotic mixing regime. If E is the energy per unit volume, then conservation of energy in the moving frame allows us to write

$$\frac{d}{dt}\left\{ \int_{V_o} E dV + \int_{V_1} (E_1 + E_2) dV \right\} =$$

$$\Delta A \left\{ -2\tilde{\rho}\tilde{h}(\tilde{U} - U_c) + \rho_1 h_1 (U_1 - U_c) + \right. \qquad (2)$$

$$\left. \rho_2 h_2 (U_2 - U_c) \right\} \quad ,$$

where

$$E = \rho e + \frac{1}{2}\rho |q|^2$$

$$\rho h = p + E \qquad (3)$$

$$\Delta A = \frac{BC - AD}{2} \quad .$$

Here $\vec{q}$ is the velocity relative to U_c. Throughout we will assume that the dominant part of the kinetic energy $|q|^2$ is given simply by the square of the streamwise velocity. This is exactly true outside the mixed region and approximately so within the layer, if the usual boundary layer assumptions are made. Thus

$$q^2 = (U - U_c)^2 \quad .$$

Use of the perfect gas relation allows us to write

$$\rho_i h_i = \frac{\gamma_i p_i}{\gamma_i - 1}\left[1 + \frac{\gamma_i - 1}{2} M_{c_i}^2\right] \quad . \qquad (4)$$

Then noting that E_1, E_2 are constant, and $dV_1/dt = -\Delta A U_c$, Equation (2) becomes

$$\frac{d}{dt}\int_{V_o} E dV = \Delta A \left\{ -2\tilde{\rho}\tilde{h}(\tilde{U} - U_c) + \right.$$

$$\frac{M_{c_1} a_1 p_1 \gamma_1}{\gamma_1 - 1}\left[1 + \frac{\gamma_1 - 1}{2} M_{c_1}^2\right] -$$

$$\frac{M_{c_2} a_2 p_2 \gamma_2}{\gamma_2 - 1}\left[1 + \frac{\gamma_2 - 1}{2} M_{c_2}^2\right] + \qquad (5)$$

$$\left. U_c(\rho_1 h_1 + \rho_2 h_2) - U_c(p_1 + p_2) \right\} \quad .$$

Re-employing Equation (4) to relate $\rho_i h_i$ to p_i in the last two terms on the right hand side, we write

$$\frac{d}{dt}\int_{V_o} E dV = \Delta A \left\{ -2\tilde{\rho}\tilde{h}(\tilde{U} - U_c) + \right.$$

$$\frac{M_{c_1} a_1 p_1 \gamma_1}{\gamma_1 - 1}\left[1 + \frac{\gamma_1 - 1}{2} M_{c_1}^2\right] -$$

$$\frac{M_{c_2} a_2 p_2 \gamma_2}{\gamma_2 - 1}\left[1 + \frac{\gamma_2 - 1}{2} M_{c_2}^2\right] + \qquad (6)$$

$$\frac{U_c p_1}{\gamma_1 - 1}\left[1 + \frac{\gamma_1(\gamma_1 - 1)}{2} M_{c_1}^2\right] +$$

$$\left. \frac{U_c p_2}{\gamma_2 - 1}\left[1 + \frac{\gamma_2(\gamma_2 - 1)}{2} M_{c_2}^2\right] \right\} \quad .$$

This expression simplifies greatly if we invoke the assumptions explicit to the convective Mach number concept, namely equal static pressures ($p_1 = p_2$) and equal specific heat ratios ($\gamma_1 = \gamma_2$). This allows us to combine terms and explicitly calculate $\tilde{\rho}\tilde{h}$ using the Crocco-Busemann relation (assuming the turbulent Prandtl number is 1, see Appendix A for details). This yields

$$\frac{d}{dt}\int_{V_o} EdV =$$

$$\Delta A \left\{ -\frac{M_c \gamma p}{\gamma-1}\left[1 + \frac{\gamma-1}{2} M_c^2\right](a_1 - a_2)\right.$$

$$+ \frac{M_c \gamma p}{\gamma-1}\left[1 + \frac{\gamma-1}{2} M_c^2\right](a_1 - a_2)$$

$$\left. + \frac{2U_c p}{\gamma-1}\left[1 + \frac{\gamma(\gamma-1)}{2} M_c^2\right]\right\} ,$$

or

$$\frac{d}{dt}\int_{V_o} EdV = \frac{2\Delta A U_c p}{\gamma-1}\left[1 + \frac{\gamma(\gamma-1)}{2} M_c^2\right] . \quad (7)$$

Under these assumptions the increase in energy of the mixed region exactly equals the decrease in energy of the two streams.

Defining a mixing rate m as the rate of increase of mass in the mixed volume V_o

$$m = \frac{d}{dt}\int_{V_o} \rho dV = \tilde{\rho}\frac{dV_o}{dt} = 2\tilde{\rho}\Delta A U_c , \quad (8)$$

we can integrate Equation (7) to obtain the growth of the mixing region's energy in terms of the mixing rate. Thus

$$\hat{E}_s = \int_{V_o} EdV = C_V \bar{T} m\left(1 + \frac{\gamma(\gamma-1)}{2} M_c^2\right)t , \quad (9)$$

where $\bar{T}$ is an average temperature defined by $\bar{T} = p/R\tilde{\rho}$.

Note that this expression is independent of the mechanism for mixing. In the following section we derive another relation between mixing rate and energy, but this for a specific mixing model, the vortex.

ENERGY AND MIXING OF AN ISOLATED, CONVECTING VORTEX

Consider the isolated vortex, shown in Figure 4, convecting in a uniform free stream of Mach number M_∞. The mixing rate per unit span of such a two-dimensional vortex can be defined approximately as

$$m = \int_{-x_1}^{x_1} \rho_o |v| dx , \quad (10)$$

where v is the perturbation velocity normal to the x-axis, ρ_o is the density of the free stream, and x_1 is chosen to be large enough to encompass the major influence of the vortex's velocity field. The perturbation energy of this vortex $\hat{E}_s$ is defined as

$$\hat{E}_s = \int_V \left[\rho_o e + \frac{1}{2}\rho_o \Delta q^2\right] dV , \quad (11)$$

where V is some suitably chosen control volume, and Δq is the perturbation velocity due to the vortex, related approximately to its strength Γ by $\Gamma \simeq 2\pi\Delta q r_c$ (r_c = core radius). It can be argued strictly on dimensional grounds that Γ is proportional to the root of the energy $E_s^{1/2}$. A similar proportionality holds for the mixing rate m, by identifying the perturbation velocity v approximately with Δq. As shown in Appendix B this approximation is correct provided the perturbation Mach number satisfies

$$M^2 \left(= \frac{\Delta q^2}{a_\infty^2}\right) >> \frac{\gamma-1}{2} M^4$$

If we then define a nondimensional mixing rate $\bar{m}$ by

$$\bar{m} = m/\rho_o U_o S , \quad (12)$$

where S is the area through which fluid is transported, we are able to write a scaling relation

$$\bar{m} = \bar{m}_o \left[\frac{\hat{E}_s}{\hat{E}_o}\right]^{1/2} . \quad (13)$$

Here $\bar{m}_o$ is the mixing rate associated with a reference vortex of energy $\hat{E}_o$. Equation (13) is the second relation between mixing rate and energy, but applied to a steady state vortex. Equation (9), on the other hand, relates an increasing energy to a fixed mixing rate and an expanding control volume. However, because of the slow growth of the control volume, we may assume

Equation (13) holds in the quasi-steady sense and associate $\bar{m}$ (= $m/\rho_o U_o S$) and $\hat{E}_s$ there with the corresponding quantities in the energy balance, Equation (9). This allows us to eliminate $\hat{E}_s$ from Equation (9) and write

$$\bar{m} = \frac{\bar{m}_o^2}{\hat{E}_o} C_V \bar{T} \left(1 + \frac{\gamma(\gamma-1)}{2} M_c^2\right) \rho_o U_o S t \qquad (14)$$

The quasi-steady assumption is equivalent to replacing $\hat{E}_s$, $\hat{E}_o$ in Equation (13) by their nondimensional counterparts $\bar{E}_s$, $\bar{E}_o$, where

$$\bar{E}_o = \frac{\hat{E}_o}{E_\infty \rho_o V} \quad , \qquad (15)$$

$$E_\infty = C_V T_\infty + \frac{1}{2} U_\infty^2 = \qquad (16)$$

$$C_V T_\infty \left(1 + \frac{\gamma(\gamma-1)}{2} M_\infty^2\right) \quad ,$$

and V is now recognized as the slowly growing control volume V_o of the original energy balance, Equation (2). This returns Equations (13) and (14) to a form where mixing rate $\bar{m}$ is constant.

What is the most appropriate choice for the scale quantities T_∞ and M_∞^2 in Equation (16)? In the frame of reference moving with the vortices the mixed layer has temperature $\bar{T}$, and the oncoming free streams are at a Mach number of M_c. Picking these as reference values, and also choosing $U_o S$ in Equation (12) such that

$$U_o S = V \quad , \qquad (17)$$

we obtain

$$\bar{m} = \frac{\bar{m}_o^2}{\bar{E}_o} \quad . \qquad (18)$$

This equation, one of the primary results of the paper, shows that the nondimensionalized mixing rate of the shear layer $\bar{m}$ can be related to the nondimensionalized mixing $\bar{m}_o$ of an isolated vortex, of energy $\bar{E}_o$, fed by an oncoming flow at the convective Mach number M_c. This allows us to obtain the variation of shear layer mixing with M_c by examining the corresponding variation for an isolated vortex. In the next section we obtain this variation analytically after a novel substitution which replaces the reference, isolated vortex with the bound circulation of a thin lifting airfoil.

THE AIRFOIL ANALOGY

As shown in Appendix B, the energy E_o of a vortex is proportional to its rotational kinetic energy (RKE), provided any temperature perturbations are due solely to the velocity field. Thus we may rewrite the equivalence relation, Equation (18), as

$$\bar{m} = \frac{\bar{m}_o^2}{\eta (RKE)_o} \quad , \qquad (19)$$

where η is some proportionality constant.

If we now wish to obtain the ratio of nondimensional mixing at M_c to its incompressible counterpart ($M_c = 0$), we write

$$\frac{\bar{m}}{\bar{m}_i} = \left[\frac{m_o}{m_{oi}}\right]^2 \left[\frac{(RKE)_{oi}}{(RKE)_o}\right] \quad , \qquad (20)$$

where the subscript i stands for incompressible conditions. It is this quantity, plotted from the experimental data, which most clearly shows the effects of decreased mixing as M_c increases.

Lele,[9] among others, has noted that the flow field around the rollers in a two-dimensional shear layer for $M_c > .6$ bears a strong resemblance to that about a transonic airfoil. We can obtain an analytic representation of the right hand side of the above mixing ratio equation by invoking this similarity. Assume that the isolated reference vortex in a freestream of $M = M_c$ can be replaced by the bound circulation produced by a thin lifting airfoil at constant angle of attack. Then in the context of thin airfoil theory we may solve the Prandtl-Glauert equation for both the mixing m_o, defined similar to Equation (10), and the rotational kinetic energy $(RKE)_o$, as a function of the Mach number. The details are shown in Appendix C. The result for the mixing ratio is

$$\frac{\bar{m}}{\bar{m}_i} = \frac{(1 - M_c^2)^{3/2}}{(1 - M_c^2/2)} \qquad (21)$$

This relation is plotted in Figure 5, along with the data of Papamoschou and Roshko, their transcription of Bogdanoff's own compendium, and two points from

Samimy and Elliott. Papamoschou and Roshko's earlier data (AIAA 86-0162) were based on visual thickness judged from schlieren pictures, while their later data comes from pitot surveys of the shear layers. For convective Mach numbers less than .8, Equation (21) captures the correct qualitative trend of mixing decrease and goes right through the experimental scatter. Numerical integration of the airfoil problem using the nonlinear, transonic small disturbance equation for the higher range of Mach numbers does not substantially alter the shape of the mixing ratio curve, except very near $M_c = 1$. This effect can be seen as the dotted curve in the figure.

What are the physical effects embodied in Equation (21)? One can immediately identify the downwash due to the airfoil with the entrainment velocity of the layer. For simplicity of analysis we have kept downwash constant and shown that the rotational kinetic energy due to this downwash decreases with M_c. In a mixing layer at a given velocity ratio it is perhaps more physical to say that rotational kinetic energy is kept constant (being essentially a function of the velocity difference) and that entrainment velocity (downwash) decreases with M_c. Either way the decrease is seen to be a function of the compressibility parameter $1 - M^2$. The large structures have an induced velocity field which attempts to deflect fluid from the freestreams into the layer. As convective Mach number increases, the energy of this field goes increasingly into compression of the fluid *as it is deflected*, and not just into deflection, as it does for the incompressible case.

Our physical explanation of the mixing decrease is at variance with that suggested previously.[9] We agree that compressibility is the source of the decrease (baroclinic torques play no part), but disagree on how its effects are manifested. It is important to remember that the airfoil analogy employs potential theory to obtain its analytical expression for the mixing decrease. Thus it ascribes decreased mixing to *irrotational* effects. This is in sharp distinction to Lele's explanation, which is based on arguments concerning vorticity redistribution.

THREE-DIMENSIONAL EFFECTS: SWEPT OR BIFURCATING VORTICES

The predictions of Equation (21) for mixing ratio decrease clearly break down for $M_c > .7$-.8. It is in this Mach number range that two-dimensional numerical simulations show shocks forming on the spanwise vortices. However, experimental evidence for the appearance of such shocks in real shear layers is lacking. In recent work by Papamoschou,[11] which postulated the existence of shocks to explain discrepancies between measured and theoretical values of M_c, visual evidence for them in Schlieren pictures could not be found.

It is our conjecture that for $M_c > .7$-.8 three-dimensional flow becomes increasingly important in the mixing layer, and that the flow adjusts itself through this third dimension so as to avoid shock formation. We do not know if this can be enunciated as a general principle, but we can point immediately to a celebrated example, the transonic area rule due to Whitcomb,[12] in which allowance for cross flow delays appearance or weakens shocks. In the case of the shear layer we suggest two possible scenarios for three-dimensionality: vortex sweep or vortex bifurcation. In either case inclusion of these effects in the original analysis predicts leveling off of the mixing ratio curve at the critical Mach number where three-dimensionality begins. The theory does not predict what this Mach number will be; it must be gotten from experiment or simulation.

Consider the swept vortex arrangement, shown in plan, on Figure 6. Here the mixers are aligned at some angle, θ, to the cross stream direction. Figure 3 is still valid if the x coordinate is aligned normal to the structures rather than to the shear layer flow direction.

Since the quantity m in the control volume analysis is nondimensionalized by the plan area S, the analysis for the swept vortex is the same as for the unswept case except that the reference vortex related to m_o is now in a flow with Mach number M_c and swept at angle θ to this flow. Since from swept wing theory only the Mach number normal to the vortex is important in calculating $|v|$, m_o is calculated for a vortex in a flow with a Mach number of $M_c \cos\theta$. If M^* denotes the critical value of M_c at which shock waves start to appear, and if the vortex sweeps so as to avoid shock waves, then

$$M^* = M_c \cos\theta \quad , \tag{22}$$

and it follows that both $\bar{m}_o$ and $(RKE)_o$ in Equation (20) will remain fixed at their value at M^*. Consequently $\bar{m}/\bar{m}_i$ will remain frozen at its critical value ($M_c = M^*$) when $M_c > M^*$. The sweep assumption may break down for Mach numbers much greater than M^* because of nonlinearity, but it is expected that the analysis given above will be valid for low supersonic values of M_c. The value of M^* remains to be decided. If a value of 0.77 is taken, then the results shown in Figure 5 as the chain dash line can be obtained. This value is in the range predicted by numerical simulations $0.7 < M < 0.8$ and is the subject of further study.

A similar effect is calculated if it is assumed that the spanwise vortices bifurcate into a mixture of spanwise and streamwise vortices such as sketched in plan view on Figure 7. This geometry could simply be a strengthening of the roller-braid structure observed in subsonic mixing layers. As is shown in Appendix D, the total energy, E, in this system can be found from Equations (D1-D4) and gives

$$E = \left\{ \frac{\tilde{m}}{\tilde{E}_o^{1/2}} \alpha^{1/2} + \frac{\hat{m}_o}{\hat{E}_o^{1/2}} (1 - \alpha)^{1/2} \right\}^2, \quad (23)$$

where the caret ($\hat{}$) refers to the streamwise vortex, the tilde ($\tilde{}$) to the spanwise vortex, and α is a measure of the partition of energies between the two vortices. The velocity in the spanwise vortex is proportional to the strength of the vortex, which in turn is proportional to $\tilde{E}^{1/2}$. If the peak velocity in this vortex is to be held at sonic speed (critical value), then it follows that

$$E^* = \left(\frac{\tilde{m}_o^*}{\tilde{E}_o^{*1/2}} \right)^2 , \quad (24)$$

where "*" denotes a value at the convective Mach number M^* at which the spanwise vortex has a sonic peak velocity.

From Equation (D4)

$$\alpha E^* = E , \quad (25)$$

and hence from Equations (23) and (24)

$$\alpha = \left(\frac{\tilde{m}_o^*}{\tilde{E}_o^{*1/2}} \right)^2 \Big/ \left\{ \frac{\tilde{m}_o}{\tilde{E}_o^{1/2}} \alpha^{1/2} + (1 - \alpha)^{1/2} \frac{\hat{m}_o}{\hat{E}_o^{1/2}} \right\}^2 . \quad (26)$$

Using Equation (D4) it follows from Equation (26) that

$$\alpha = \left(\frac{\tilde{m}_o^*}{\tilde{E}_o^{*1/2}} \right)^2 \Big/ \bar{m} \quad (27)$$

or, using Equation (18)

$$\alpha = \left(\frac{\bar{m}^*}{\bar{m}_i} \right) \Big/ \left(\frac{\bar{m}}{\bar{m}_i} \right) , \quad (28)$$

where $\bar{m}_i$ is the value of m at incompressible speeds.

Since the spanwise vortex does not change character with Mach number, it follows that in Equation (D16) (using Equation (18))

$$\frac{\hat{m}_o^2}{\hat{E}_o} = \bar{m}_i . \quad (29)$$

Consequently, Equation (D16) can be written as

$$\frac{\bar{m}}{\bar{m}_i} = \left\{ \left(\frac{\bar{m}}{\bar{m}_i} \right)^{1/2} \alpha^{1/2} + (1 - \alpha)^{1/2} \right\}^2 . \quad (30)$$

Equations (28) and (30) are two equations for $\bar{m}/\bar{m}_i$ and α in terms of $\bar{m}^*/\bar{m}_i$. If the critical Mach number is taken to be 0.77, then this theory gives the result shown in Figure 5 as the dashed line.

CONCLUSIONS

We have presented a theory, free from linear instability arguments, which quantitatively predicts the decreased mixing rates observed in compressible free shear layers. The primary mechanism underlying this decrease is the attenuating effect compressibility has on the large scale structures' ability to deflect fluid away from the free streams and into the mixing layer. The flow energy available for entrainment, which comes from the induced velocity field of the structures, is now partitioned between deflection and compression work that occurs during deflection. This is an irrotational effect. Thus, there is no connection between this mechanism and the attenuation of vorticity redistribution scheme proposed by Lele. In incompressible layers, "pushing" on the free stream fluid moves it into the layer; in compressible layers, "pushing" results in some compression also, and thus less deflection. This phenomenon is explicit in the airfoil analogy, where a constant downwash results in decreasing rotational kinetic energy as M_c increases (or alternatively, if rotational energy is held constant as M_c increases, the downwash must decrease).

Reduced linear instability is not the cause of reduced shear layer mixing. Rather both are manifestations of the retarding effects of compressibility. To enhance mixing one must decrease the effects of compressibility, not attempt to increase linear instability. Even if initial instability were somehow enhanced, the long term growth of structures would still be subject to the attenuating effects of compressibility. This is probably one of the reasons why trailing edge treatments have little or no effect on compressible mixing.

Compressibility effects can be reduced by assuming the flow becomes three dimensional. Our theory suggests that adjustment of the flow in this manner, in a way that avoids shocks at high values of M_c, explains the levelling of the growth rate curve for

M_c > .7-.8. Indeed, it appears that Nature has already found a mechanism to keep mixing finite. Without the alternative of three-dimensional flow, mixing would decrease still further, the energy available for mixing having been further dissipated by shocks. A difference in the amount of flow three-dimensionality from facility to facility may explain some of the experimental scatter in the literature. There is certainly wide variation in the aspect ratio of the test sections of the various tunnels.

ACKNOWLEDGEMENTS

This work was supported by the Air Force Office of Scientific Research under contract F49620-88-C-0003. The US Government is authorized to reproduce and distribute reprints for Governmental purposes notwithstanding any copyright notation thereon.

REFERENCES

1. Papamoschou, D. and Roshko, A., "The Compressible Turbulent Shear Layer: An Experimental Study," Journal of Fluid Mechanics, Vol. 197, p. 453, 1988.

2. Bogdanoff, D. W., "Compressibility Effects in Turbulent Shear Layers," AIAA Journal, Vol. 21, no. 6, p. 926, 1983.

3. Samimy, M. and Elliott, G. S., "Effects of Compressibility on the Structure of Free Shear Layers," AIAA 88-3054A, 1988.

4. Messersmith, N. L., Goebel, S. G., Frantz, W. H., Krammer, E. A., Renie, J. P., Dutton, J. C., and Krier, H., "Experimental and Analytical Investigations of Supersonic Mixing Layers," AIAA 88-0702, 1988.

5. Gutmark, E., Schadow, K. C., and Wilson, K. J., "Mixing Enhancement in Coaxial Supersonic Jets," AIAA 89-1812, 1989.

6. Brown, G. L. and Roshko, A., "On Density Effects and Large Structures in Turbulent Mixing Layers," Journal of Fluid Mechanics, Vol. 64, p. 775, 1974.

7. Gropengiesser, H., "Study of the Stability of Boundary Layers in Compressible Fluids," NASA TT-F-12, p. 786.

8. Sandham, N. and Reynolds, W. C., "The Compressible Mixing Layer: Linear Theory and Direct Simulation," AIAA 89-0371, 1989.

9. Lele, S., "Direct Numerical Simulation of Compressible Free Shear Flows," AIAA 89-0374, 1989.

10. Thompson, K. W., "Time Dependent Boundary Conditions for Hyperbolic Systems," Journal of Computational Physics, Vol. 68, p. 1, 1987.

11. Papamoschou, D., "Structure of the Compressible Turbulent Shear Layer," AIAA 89-0126.

12. Whitcomb, R. T., "A Study of Zero-Lift Drag-Rise Characteristics of Wing Body Combinations Near the Speed of Sound," NACA Report 1273, 1956.

APPENDIX A

The Crocco-Busemann relation for turbulent Prandtl number $P_t = 1$ regulates the temperature field in a boundary layer to be strictly a function of the streamwise velocity U'

$$C_p T = -\frac{(U'-C_1)^2}{2} + C_2 \,, \qquad \text{(A1)}$$

where with boundary condition $T = T_1$ at $U' = U'_1$, and $T = T_2$ at $U' = U'_2$ we obtain

$$C_1 = \frac{U'_1 + U'_2}{2} + \frac{C_p(T_1 - T_2)}{(U'_1 - U'_2)}$$

$$C_2 = \frac{1}{2}\left\{ \left[\frac{U'_1 - U'_2}{2} \right]^2 + \right. \qquad \text{(A2)}$$

$$\left. C_p(T_1 + T_2) + \left[\frac{C_p(T_1 - T_2)}{(U'_1 - U'_2)} \right]^2 \right\} .$$

If we assume a velocity profile in the U_c frame

$$U'(y) = \frac{U'_1 + U'_2}{2} + \frac{U'_1 - U'_2}{2} \tanh y - U_c$$

$$= \frac{(U'_1 - U'_c) + (U'_2 - U'_c)}{2} +$$

$$\frac{(U'_1 - U'_c) - (U'_2 - U'_c)}{2} \tanh y \qquad \text{(A3)}$$

$$= \frac{U_1 + U_2}{2} + \frac{U_1 - U_2}{2} \tanh y$$

$$U_1 = U'_1 - U_c \quad \text{etc.} \,,$$

we can calculate the temperature distribution, and from that the density distribution using the perfect gas law.

Similarly, using the relation

$$h = C_p T + \frac{U^2}{2} \qquad \text{(A4)}$$

we can obtain h(y). Then to evaluate the average value of $\tilde{\rho}\tilde{h}$ across the layer we write

$$\tilde{\rho}\tilde{h} = \frac{1}{2L} \int_{-L}^{L} \rho(y)\, h(y)\, dy$$

$$= \frac{1}{2L} \frac{\gamma p}{\gamma - 1} \quad x \qquad \text{(A5)}$$

$$\int_{-L}^{L} \frac{A\cosh^2 y + 2B\sinh y \cosh y}{a\cosh^2 y + 2b\sinh y \cosh y + c\sinh^2 y}\, dy \,,$$

where

$$A = \frac{C_p(T_1 + T_2)}{2} + \frac{U_1^2 + U_2^2}{4}$$

$$B = \frac{C_p(T_1 + T_2)}{4} + \frac{(U_1^2 - U_2^2)}{8}$$

$$a = \frac{C_p(T_1 + T_2)}{2} + \frac{1}{2}\left[\frac{U_1 - U_2}{2} \right]^2 \qquad \text{(A6)}$$

$$b = \frac{C_p(T_1 - T_2)}{4}$$

$$c = -\frac{1}{2}\left[\frac{U_1 - U_2}{2} \right]^2 .$$

This integral may be evaluated with the aid of formula 2.452.2, page 111, Gradshteyn and Ryzhik, "Table of Integrals, Series, and Products," Academic Press, 1980.

$$\widetilde{\widetilde{\rho h}} = \frac{1}{2L}\frac{\gamma p}{\gamma - 1}\frac{1}{4b^2 - (a + c)^2}$$

$$\Big\{[4Bb - A(a + c)]2L +$$

$$[Ab - B(a + c)]\log_e$$

$$\left[\frac{a + 2b\tanh L + c\tanh^2 L}{a - 2b\tanh L + c\tanh^2 L}\right] \qquad \text{(A7)}$$

$$+ \frac{2Ab^2 - 2B(a - c) - Ac(a + c)}{2\sqrt{b^2 - ac}}\log_e$$

$$\left[\frac{\left(c\tanh L + b - \sqrt{b^2 - ac}\right)}{\left(c\tanh L + b + \sqrt{b^2 - ac}\right)}\right.$$

$$\left.\frac{\left(-c\tanh L + b + \sqrt{b^2 - ac}\right)}{\left(-c\tanh L + b - \sqrt{b^2 - ac}\right)}\right]\Big\}$$

As L becomes large the second and third bracketed terms go to finite values and thus make negligible contribution to $\widetilde{\widetilde{\rho h}}$. Evaluation of the first term gives

$$\widetilde{\widetilde{\rho h}} = \frac{\gamma p}{\gamma - 1}\left\{1 + \frac{U_1^2}{4C_p T_1} + \frac{U_2^2}{4C_p T_2}\right\} = \qquad \text{(A8)}$$

$$\frac{\gamma p}{\gamma - 1}\left\{1 + \frac{\gamma - 1}{4}\frac{U_1^2}{a_1^2} + \frac{\gamma - 1}{4}\frac{U_2^2}{a_2^2}\right\} .$$

However,

$$\frac{U_1^2}{a_1^2} = \left[\frac{U'_1 - U_c}{a_1}\right]^2 = M_c^2 = \left[\frac{U'_2 - U_c}{a_2}\right]^2 = \frac{U_2^2}{a_2^2} ,$$

so

$$\widetilde{\widetilde{\rho h}} = \frac{\gamma p}{\gamma - 1}\left\{1 + \frac{\gamma - 1}{2}M_c^2\right\} . \qquad \text{(A9)}$$

Note that this result is largely independent of the assumed form of the velocity profile between the two streams, provided L is large compared to the layer thickness.

APPENDIX B

The energy due to the vortex is given by

$$E = C_v(T - T_\infty) + \tfrac{1}{2}(q - q_\infty)^2 , \qquad \text{(B1)}$$

where "∞" denotes ambient conditions and q is the velocity.

From the isentropic relations the temperature due to the local Mach number of the vortex is

$$\frac{T}{T_\infty} = \left[1 + \frac{(\gamma - 1)}{2}M^2\right]^{-1} , \qquad \text{(B2)}$$

where T_∞ is the stagnation temperature of the vortex (i.e., when M is zero), and M is the Mach number given by

$$M^2 = \frac{\Delta q^2}{a^2} . \qquad \text{(B3)}$$

Here

$$\Delta q^2 = (q - q_\infty)^2 , \qquad \text{(B4)}$$

and

$$a^2 = \gamma R T . \qquad \text{(B5)}$$

Equation (B2) can be expanded to give

$$\frac{T}{T_\infty} \sim 1 - \frac{(\gamma-1)}{2} M^2 + \text{---} \quad , \tag{B6}$$

so to a first approximation

$$\frac{T}{T_\infty} - 1 = - \frac{(\gamma-1)}{2} \frac{\Delta q^2}{a^2} \quad , \tag{B7}$$

where a is the local speed of sound. Also

$$a^2 = \gamma R T_\infty \left\{ \frac{T}{T_\infty} \right\} = \gamma R T_\infty [1 - \frac{(\gamma-1)}{2} M^2 \text{---}] \tag{B8}$$

$$= a_\infty^2 [1 - \frac{(\gamma-1)}{2} M^2 \text{---}] \, .$$

To a first approximation in Δq^2 then

$$\left\{ \frac{T}{T_\infty} - 1 \right\} = - \frac{(\gamma-1)}{2} \frac{\Delta q^2}{a_\infty^2} \, . \tag{B9}$$

Equation (B1) can now be written as

$$E = C_v T_\infty \left\{ \frac{T}{T_\infty} - 1 \right\} + \frac{1}{2} \Delta q^2$$

$$= C_v T_\infty \left[- \frac{(\gamma-1)}{2} \frac{\Delta q^2}{a_\infty^2} \right] + \frac{1}{2} \Delta q^2 \tag{B10}$$

$$= \frac{\Delta q}{2}^2 \frac{(\gamma-1)}{\gamma} \, .$$

Hence E is proportional to Δq^2. Since Δq is a perturbation velocity it is proportional to the strength of the vortex, Γ, and hence

$$E \propto \Gamma^2$$

Since the rotational kinetic energy is proportional to Δq^2 it follows that E is proportional to the rotational kinetic energy.

APPENDIX C

Analysis for Subsonic Flow

Consider the Prandtl-Glauert Equation

$$\beta^2 \phi_{xx} + \phi_{yy} = 0 \, , \tag{C1}$$

where ϕ is a perturbation velocity potential, such that,

$$u = \phi_x \tag{C2}$$

$$v = \phi_y \, ,$$

and u and v are normalized perturbation velocities in the x and y directions respectively. x and y are nondimensionalized to the airfoil chord, $2x_o$; β is given by

$$\beta = (1 - M_c^2)^{1/2} \quad . \tag{C3}$$

Equation (C1) can be transformed by the substitution

$$\bar{y} = \beta y \tag{C4}$$

to give Laplace's equation

$$\phi_{xx} + \phi_{yy} = 0. \tag{C5}$$

For the flow over an airfoil with lift the classic thin airfoil analysis gives

$$\Delta u (x, \bar{y}) = \frac{1}{\pi} \int_0^1 \frac{\Delta u (x, o) \bar{y}}{(x-\xi)^2 + \bar{y}^2} \, d\xi \tag{C6}$$

$$\bar{\phi}_{\bar{y}} = \frac{1}{2\pi} \int_0^1 \frac{\Delta u (x, o) (x-\xi)}{(x-\xi)^2 + \bar{y}^2} \, d\xi \quad , \tag{C7}$$

where Δu and $\phi_{\bar{y}}$ are defined by

$$\Delta u(x,\bar{y}) = \tfrac{1}{2} [u(x,\bar{y}) - u(x,-\bar{y})] \tag{C8a}$$

$$\phi_{\bar{y}}(x,\bar{y}) = \tfrac{1}{2} [v(x,\bar{y}) + v(x,\bar{y})] \, . \tag{C8b}$$

For a given angle of attack, α_o,

$$\bar{v} = -\alpha_o = \beta \bar{\phi}_{\bar{y}} \, , \tag{C9}$$

or

$$\bar{\phi}_{\bar{y}} = -\alpha_o / \beta \, . \tag{C10}$$

By putting $\bar{y} = 0$ in Equation (C7) it may be seen that

$$\Delta u(x,o) = \Delta u_i(x,o)/\beta \ , \qquad (C11)$$

where the subscript i denotes a value at incompressible speeds, that is, at $\beta = 1$. It may also be seen that

$$\bar{v}(x,\bar{y}) = \beta\bar{\phi}_{\bar{y}} = \bar{v}_i(x,\bar{y}) \qquad (C12)$$

and that, from Equation (C6),

$$\Delta u(x,\bar{y}) = \tfrac{1}{2}\Delta u_i(x,\bar{y}) \ . \qquad (C13)$$

If the mixing, m, is defined as the movement of fluid from the upper half plane to the center and vice-versa, then

$$m = \rho_\infty \left\{ \int_{-x_1}^{0} |v|_{y=0}\, dx + \int_{1}^{x_2} |v|_{y=0}\, dx \right\} \ , \qquad (C14)$$

which, using Equation (C12) gives

$$\bar{m} = \bar{m}_i \ , \qquad (C15)$$

where $\bar{m}_i$ is the mixing for incompressible flow for the same α_o.

The rotational kinetic energy (RKE) is defined in a small disturbance approximation by

$$RKE = \frac{1}{2}\rho_\infty \int_S [\Delta u^2 + \bar{v}^{\,2}]\, dxdy \ , \qquad (C16)$$

where S is half of the flow domain.

Equation (C16) can be written as

$$RKE = \frac{1}{2}\frac{\rho_\infty}{\beta} \int_S [\Delta u_i^{\,2}(x,\bar{y})/\beta^2 + \bar{v}_i^{\,2}(x,\bar{y})]\, dxd\bar{y} \ , \qquad (C17)$$

or

$$RKE = \frac{1}{\beta^3} I_1 + \frac{1}{\beta} I_2 \ . \qquad (C18)$$

Here

$$I_1 = \frac{1}{2}\rho_\infty \int_s \Delta u_i^{\,2}(x,\bar{y})\, dxd\bar{y}$$

$$I_2 = \frac{1}{2}\rho_\infty \int_s \bar{v}_i^{\,2}(x,\bar{y})\, dxd\bar{y} \ , \qquad (C19)$$

which are independent of Mach number.

Using Equations (C15) and (C18) in Equation (20) of the main text gives

$$\frac{\bar{m}}{\bar{m}_i} = \left(\frac{I_1 + I_2}{I_1 + \beta^2 I_2} \right) \beta^3 \qquad (C20)$$

If the airfoil is small compared to the extent of domains, there is no difference between $\Delta u(x,y)$ and $\bar{v}(x,\bar{y})$, that is, the airfoil resembles a point vortex. In this case

$$I_1 = I_2 \ , \qquad (C21)$$

and Equation (C20) becomes

$$\frac{\bar{m}}{\bar{m}_i} = \left[\frac{\beta^3}{1 - M_c^{\,2}/2} \right] \qquad (C22)$$

APPENDIX D

Effect of Multiple Vortices

From Equations (9) and (13) the energy $\hat{E}_s$ is given by

$$\hat{E}_s = \bar{m} C_v \bar{T} \left[1 + \frac{\gamma(\gamma - 1)}{2} M_c^{\,2} \right] \rho_o U_o St \qquad (D1)$$

where $\bar{m}$ is the mixing due to the structures. Let the mixing be caused by N vortices on the mixing line, each with a mixing rate of $\bar{m}_j$ such that

$$\bar{m} = \sum_{j=1}^{N} \bar{m}_j \ . \qquad (D2)$$

Using the scaling of Equation (13) we obtain

$$\bar{m}_j = \bar{m}_o \left(\frac{\hat{E}_{sj}}{\hat{E}_o} \right)^{1/2}, \qquad (D3)$$

where the subscript "o" denotes a mixer with energy $\hat{E}_o$, and $\hat{E}_{sj}$ is the energy associated with the jth structure. If the energy of each vortex is a fraction α_i of the total energy E_s, then

$$\hat{E}_{sj} = \alpha_j \hat{E}_s \qquad (D4)$$

and

$$\sum_{j=1}^{N} \alpha_j = 1 . \qquad (D5)$$

Using Equation (D2) - (D4) in Equation (D1) gives

$$\bar{m} = \left(\sum_{j=1}^{N} \frac{\bar{m}_o \alpha_j}{\bar{E}_o^{1/2}} \right)^2 , \qquad (D6)$$

where

$$\bar{E}_o = E_o / \left\{ C_v \bar{T} \rho_o U_o St \left[1 + \frac{\gamma(\gamma - 1)}{2} M_c^2 \right] \right\} . \qquad (D7)$$

The Mach number dependence only arises in the term $\bar{m}_o / E_o^{1/2}$ and hence the mixing will decay with Mach number no matter how many vortices there are. However, as before, this analysis neglects the viscous core of the vortices. If the vortices are small, the viscous core is larger relative to the inviscid part than in larger vortices, so overall, the mixing may not decrease as much with Mach number.

Consider now the case where there are two types of mixing structures, with mixing denoted by $\tilde{m}$ and $\hat{m}$ such that

$$\bar{m} = \sum_{j=1}^{N} \tilde{m}_j + \sum_{j=N+1}^{N_T} \hat{m}_j . \qquad (D8)$$

Again, using the scaling of Equation (13)

$$\tilde{m}_j = \tilde{m}_o \left(\frac{\tilde{E}_{Sj}}{\tilde{E}_o} \right)^{1/2}$$

$$\hat{m}_j = \hat{m}_o \left(\frac{\hat{E}_{Sj}}{\hat{E}_o} \right)^{1/2} . \qquad (D9)$$

It is assumed that the mixing is proportional to the square root of the energy of the mixer as is the case for the vortex.

Now assume that the energy of each structure is a fraction α_j of the total energy E_s and Equations (D4) and (D5) are satisfied. Use Equations (D8), (D9), and (D4) to eliminate E_s. Thus

$$\bar{m} = \left\{ \sum_{j=1}^{N} \frac{\tilde{m}_o}{\tilde{E}_o^{1/2}} \alpha_j + \sum_{j=N+1}^{N_T} \alpha_j \frac{\hat{m}_o}{\hat{E}_o^{1/2}} \right\}^2 , \qquad (D10)$$

where

$$\bar{\tilde{E}}_o = \tilde{E}_o / \left\{ C_v \bar{T} \rho_o U_o St \left[1 + \frac{\gamma(\gamma - 1)}{2} M_c^2 \right] \right\}$$

$$\bar{\hat{E}}_o = \hat{E}_o / \left\{ C_v \bar{T} \rho_o U_o St \left[1 + \frac{\gamma(\gamma - 1)}{2} M_c^2 \right] \right\} . \qquad (D11)$$

In order to alter the effect of Mach number on the mixing, the typical term

$$\frac{m_o}{\bar{E}_o^{1/2}}$$

must be less dependent on the Mach number than is the case for the simple vortex.

Note that the structure denoted by the caret can be regarded as the viscous core and that denoted by a tilde

can be regarded as the inviscid part of the vortex which decreases rapidly as $M_c \longrightarrow 1$.

If the structure denoted by a caret is a vortex with a streamwise axis, then the transonic small disturbance equation gives the potential associated with the vortex as

$$(1 - M_c^2 - k\phi_x)\phi_{xx} + \phi_{yy} + \phi_{zz} = 0, \qquad \text{(D12)}$$

where

$$k = [3 + (\gamma - 2)M_c^2]M_c^2 \quad . \qquad \text{(D13)}$$

If the vortex is uniform or nearly uniform along its axis, then the x derivatives in Equation (D12) are negligible and

$$\phi_{yy} + \phi_{zz} = 0, \qquad \text{(D14)}$$

which has no dependence on M_c. Thus the mixing associated with a vortex aligned in the streamwise direction does not decay as $M_c \longrightarrow 1$. Furthermore, there are no shock waves associated with this vortex and hence no increase in entropy.

In contrast, for a spanwise vortex the potential equation is

$$(1 - M_c^2 - k\phi_x)\phi_{xx} + \phi_{yy} = 0, \qquad \text{(D15)}$$

which can give shock waves and hence an entropy increase.

Consider now the mixing given by Equation (D10) for a single vortex and a single streamwise vortex. Thus

$$m = \left\{ \frac{\tilde{m}_o}{\tilde{E}_o^{1/2}} \alpha + (1 - \alpha) \frac{\tilde{m}_o}{\hat{E}_o^{1/2}} \right\}^{1/2} \qquad \text{(D16)}$$

where α is a measure of the partition of the energy between the vortices.

It is a reasonable hypothesis that the flow will try to develop so that entropy increases are kept to a minimum. Hence, as M_c increases, the fraction α will get smaller and the size of the spanwise vortex will decrease while the streamwise vortex will increase. This effect is in addition to the inviscid decay of the spanwise vortex noted earlier.

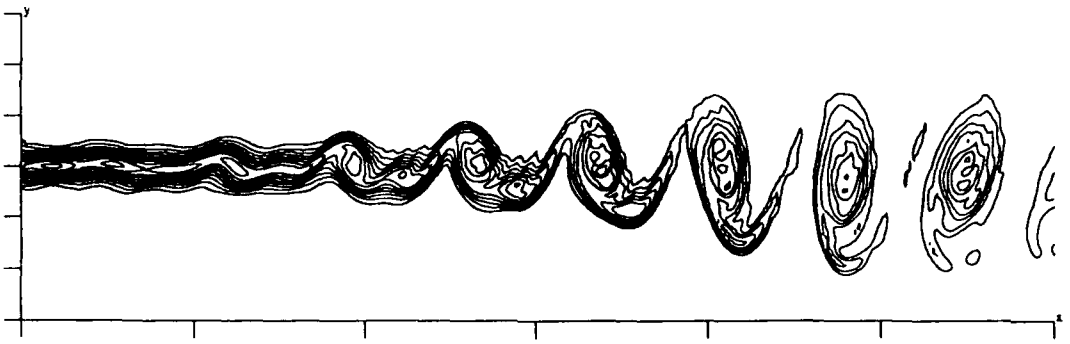

FIGURE 1. Vorticity contours in a two–dimensional mixing layer. $M_1 = 2.0$, $M_2 = 1.2$, $M_c = .4$.

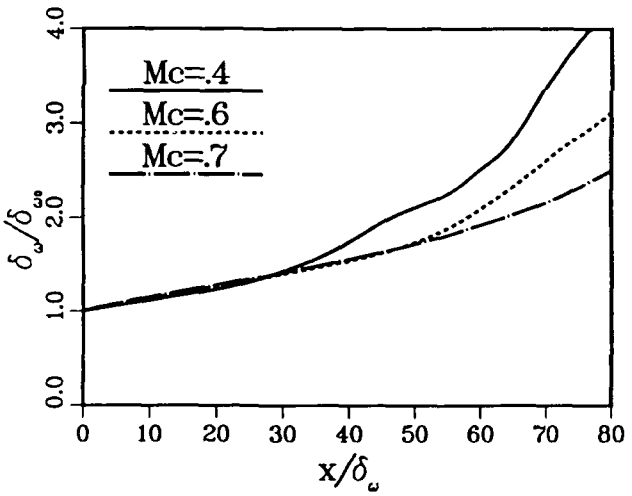

FIGURE 2. Initial spreading rates of forced two–dimensional shear layers at various convective Mach numbers

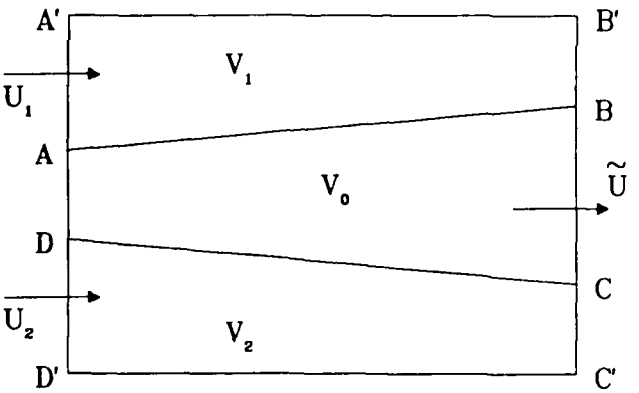

FIGURE 3. Control volume for energy balance in a shear layer.

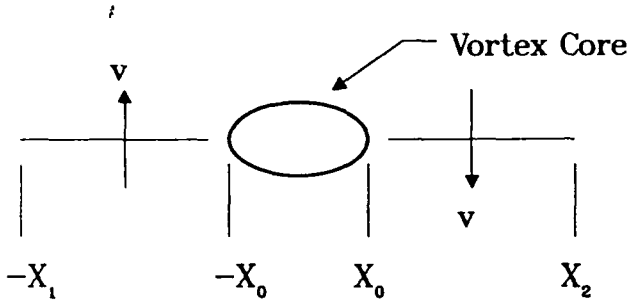

FIGURE 4. Isolated vortex model

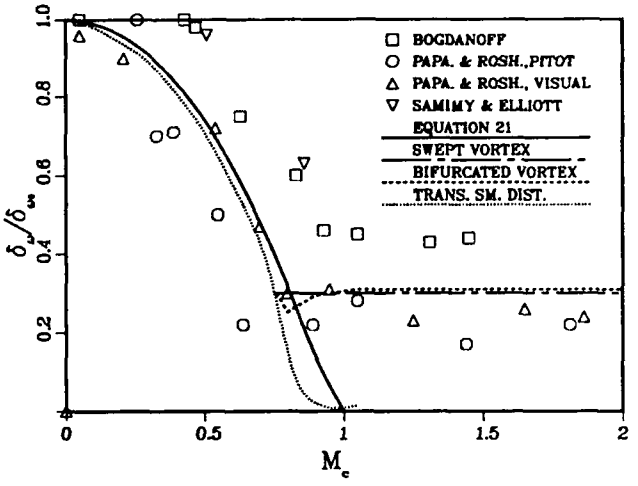

FIGURE 5. Experimentally measured layer growth rates compared to two- and three-dimensional theory.

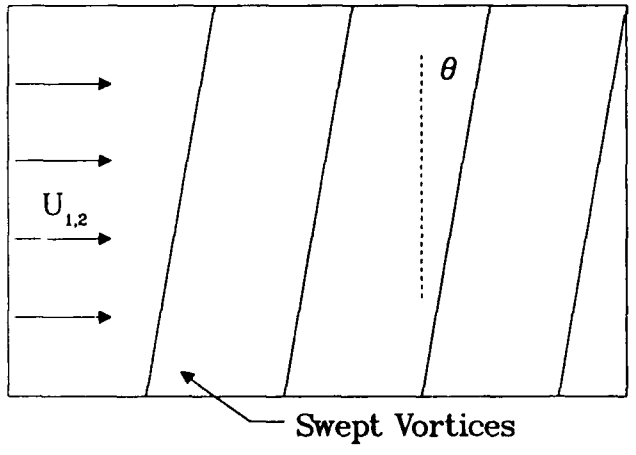

FIGURE 6. Plan view of swept vortices

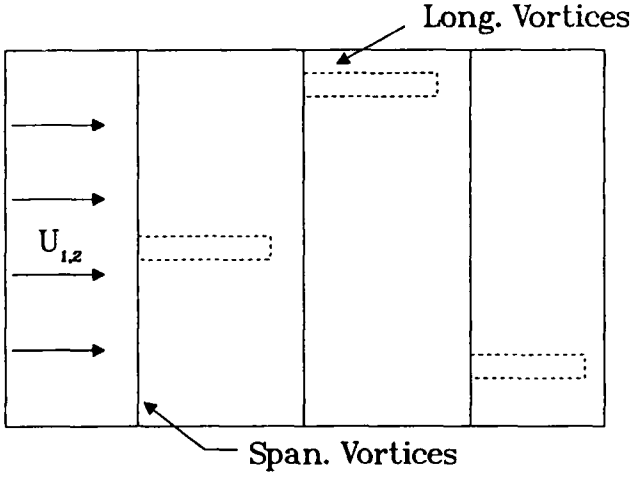

FIGURE 7. Plan view of mixture of spanwise and streamwise vortices